EFDA–JET–CP(12)03/03

A. Neto, D. Alves, B.B. Carvalho, G. De Tommasi, R. Felton, H. Fernandes,
P.J. Lomas, F. Maviglia, F.G. Rimini, F. Sartori, A.V. Stephen,
D.F. Valcárcel, L. Zabeo and JET EFDA contributors

A Real-Time Architecture for the Identification of Faulty Magnetic Sensors in the JET Tokamak

A Real-Time Architecture for the Identification of Faulty Magnetic Sensors in the JET Tokamak

A. Neto[1], D. Alves[1], B.B. Carvalho[1], G. De Tommasi[2], R. Felton[3], H. Fernandes[1], P.J. Lomas[3], F. Maviglia[2], F.G. Rimini[2], F. Sartori[4], A.V. Stephen[3], D.F. Valcárcel[1], L. Zabeo[5] and JET EFDA contributors*

JET-EFDA, Culham Science Centre, OX14 3DB, Abingdon, UK

[1]Associação EURATOM/IST, Instituto de Plasmas e Fusão Nuclear - Instituto Supérior Tecnico - Universidade Técnica de Lisboa, 1049-001 Lisboa, Portugal
[2]Associazione EURATOM/ENEA/CREATE,Università di Napoli Federico II, 80138 Napoli, Italy
[3]EURATOM-CCFE Fusion Association, Culham Science Centre, OX14 3DB, Abingdon, OXON, UK
[4]Fusion for Energy, 08019 Barcelona, Spain
[5]ITER Organisation, 13108 St. Paul-Lez-Durance, France
** See annex of F. Romanelli et al, "Overview of JET Results", (23rd IAEA Fusion Energy Conference, Daejon, Republic of Korea (2010)).*

Preprint of Paper to be submitted for publication in Proceedings of the
18th IEEE-NPSS Real-Time Conference, Berkeley, California, USA
11th June 2012 - 15th June 2012

ABSTRACT

In a tokamak, the accurate estimation of the plasma boundary is essential to maximise the fusion performance and is also the first line of defence for the physical integrity of the device. In particular, the first wall components might get severely damaged if over-exposed to a high plasma thermal load.

The most common approach to calculate the plasma geometry and related parameters is based in a large set of different types of magnetic sensors. Using this information, real-time plasma equilibrium codes infer a flux map and calculate the shape and geometry of the plasma boundary and its distance to a known reference (e.g. first wall). These are inputs to one or more controllers capable of acting on the shape and trajectory based in pre-defined requests.

Depending on the device, the error of the estimated boundary distance must usually be less than 1 centimetre, which translates into very small errors on the magnetic measurement itself. Moreover, asymmetries in the plasma generated and surrounding magnetic fields can produce local shape deformations potentially leading to an unstable control of the plasma geometry.

The JET tokamak was recently upgraded to a new and less thermally robust all-metal wall, also known as the ITER-like wall. Currently the shape controller system uses the output of a single reconstruction algorithm to drive the plasma geometry and the protection systems have no input from the plasma boundary reconstruction. These choices are historical and were due to architectural, hardware and processing power limitations.

Taking advantage of new multi-core systems and of the already proved robustness of the JET real-time network, this paper proposes a distributed architecture for the real-time identification of faults in the magnetic measurements of the JET tokamak. Besides detecting simple faults, such as short-circuits and open-loops, the system compares the expected measurement at the coil location and the real measurement, producing a confidence value. Several magnetic reconstructions, using sensors from multiple toroidally distributed locations, can run in parallel, allowing for a voting or averaging scheme selection. Finally, any fault warnings can be directly fed to the real-time protection sequencer system, whose main function is to coordinate the protection of the JET's first wall.

1. INTRODUCTION

In a tokamak, the magnetics diagnostic is a key element for the real-time feedback control of the plasma current and geometry and in the amelioration of plasma instabilities. These kind of diagnostics require the availability of a large quantity of reliable, accurate and spatially resolved magnetic sensors.

In order to compute the plasma boundary flux and thus estimate the plasma shape the XLOC [1] algorithm solves the Grad-Shafranov [2] equation in the vacuum using high degree polynomials as an approximation of the flux function. By interpolating the measurements of several magnetic probe classes (pick-up, saddles and flux loops), XLOC uses a least-squares fit method to calculate the polynomial coefficients of the different flux functions and to generate a flux map. Comparing the flux along predefined paths, also known as gaps, the Felix code [3] computes the plasma shape and other important geometrical parameters. Fig. 1 shows the definition of some of the most important gaps.

When the plasma last closed flux surface touches one of the machine physical limiters, the last closed surface flux is defined by the limiter flux and the plasma is said to be in a limiter phase. Otherwise, the boundary can be reconstructed by searching for the location of the point where $B_r = B_z = 0$, also named X-point, and its flux. In this configuration the plasma power can be significantly increased without risking the damage of the plasma facing components. This is even more important as the JET tokamak was recently upgraded to a new and less thermally robust all-metal wall, also known as the ITER-like wall (ILW). In the context of this upgrade a new protection system, named Real-time Protection Sequencer (RTPS), was developed and successfully deployed [4]. The RTPS system enables coordinated stop responses, in the form of plasma geometry and additional heating references, to fault events that are propagated using the ATM based Real-Time Data Network (RTDN) [5].

At JET the axisymmetric magnetic control of the plasma [6] in provided by the Plasma Position and Current Control (PPCC) system, composed by the shape controller and the vertical stabilisation system [7], deployed in two separate controller schemes. The former is responsible for the control of the current in 9 circuit actuators, the plasma current, the plasma position and the plasma shape, specified as a collection of gaps. The latter guarantees, in a faster time-scale and with a dedicated power supply and controller hardware, that the vertical instability due to the elongated nature of the plasma is actively controlled.

The most important measurement coil sets for the PPCC feedback control are the internal discrete coils (IDC), the saddle coils and the full flux loops. The IDC and the saddle coils provide a direct measurement of the tangential and normal components of the poloidal magnetic field along a contour defined by the magnetic vessel. Two full flux loops, located at precise poloidal positions and wound around the JET central axis, enable the direct measurement of the poloidal flux in these poloidal locations. The tokamak also contains hundreds of other pick-up coils, some optimized for higher bandwidths, on key locations, like the divertor region or the first wall poloidal limiters (see Fig. 1). A subset of these coils is used for the real-time controllers and the remaining for post-pulse physics analysis. Furthermore, the JET vessel is divided in 8 sections, also known as octants, so that equivalent coils installed in the same poloidal position, but in different octants, should provide equivalent measurements (assuming a perfect toroidal axisymmetry).

2. MAGNETICS DISTRIBUTION ARCHITECTURE

The major data acquisition systems for the magnetic sensors are named KC1D, KC1E and KC1M. The latter is used for the fast data acquisition of the high bandwidth probes for post-pulse offline analyses. The former, besides providing data storage of the magnetic signals, are the magnetic data sources of the real-time network. In particular, KC1D and KC1E distribute the same equivalent sensor, i.e. installed in the same poloidal position, using sources from different octants (mainly 3 or 7 for KC1D and 1 or 5 for KC1E). Even if two equivalent sensors are available, each system only transmits one and the consumer algorithms have no run-time information about the selected sourcing octant. This allows to change the source sensor without disturbing the consumer configurations, e.g. KC1D broadcasts the CZ01 probe, which can be set to be either C301 or C701, the probes for the poloidal position 1, from octants 3 and 7 respectively. Furthermore, each of these systems provides independent calculations of the plasma current and of the current centroid horizontal and vertical positions.

The most important consumer of this data is the shape controller system, as it uses a subset of the magnetic probes data as input to the XLOC algorithm and to independently calculate the plasma current and the centroid position. As a trustworthy and robust value of the plasma current is essential for the safe exploitation of the machine, the first function of the shape controller system is to compare the values of all the available plasma current estimations and trigger the interlock system in case of major discrepancies. Currently KC1D is used as the main data source for the XLOC model of the plasma shape feedback loop, while the KC1E data is only used as an alternative when KC1D is not available. Both KC1D and KC1E output data to the ATM network at a 500 Hz rate.

Other magnetics data real-time consumers are the WALLS system [8], responsible for the protection of the first wall against excessive power deposition, the BetaLi, which calculates the plasma energy and internal inductance and the EQUINOX [9] system, enabling the calculation of the plasma current density profile. Each of these software modules runs its own version of the Felix code, sharing the same settings for the XLOC algorithm. One of the issues relates to the maintenance and synchronisation of the XLOC configurations, common to all the projects, as any update (due for instance to the unavailability of a sensor) must be approved and propagated following a stringent set of procedures to all the modules. The real-time central controller (RTCC) provides an environment for the development of simple controllers based on experimental data and would also benefit from a validated plasma shape.

The other major consumer of magnetics data is the vertical stabilisation system which, due to its much faster control time-scale, has its own dedicated fast data acquisition system [10] connected to the sensors.

3. MAGNETICS FAULT DETECTION

Currently the detection of faults in a magnetic sensor is performed by running off-pulse algorithms. The faults can be divided in two sets: permanent and intermittent. The former requires either a physical replacement of the sensor, the fixing of the electronics connected to the sensor or an update to the algorithms responsible for performing live compensation against erroneous pick-ups and for transmitting the data to the real-time network. When a fault is found, if the coil was being used as an input to the XLOC algorithm and there is no available backup sensor, the configuration must be updated across all instances of the algorithm.

Hardware faults normally translate into a measured signal that is radically different from the signals on the neighbour coils and from the probes that are in the same poloidal location but in a different octant. Faults related to wrong compensations and software problems usually are not so evident and can be hard to diagnose. In any of the cases, the usage of faulty sensors will likely translate into dangerous plasma shape control problems that greatly increase the risk of damaging machine components. As depicted in Fig. 2, in JET pulse #80912 a software fault in the magnetics diagnostic generated a wrong compensation, against the poloidal components induced by the toroidal magnetic field coils, for the P804A coil value sent to the real-time network. This translated into an erroneous control of the horizontal distance to the first wall in the order of 1 cm. Nevertheless, during the experiment it was extremely hard to diagnose the fault since the feedback loop of the shape controller, acting on an wrong measurement, assumed to be keeping a constant distance, when in reality it was pushing the plasma against the inner wall.

Having an equivalent probe located in the same poloidal position at different toroidal locations allows to have a first order approximation of the measurement status, using a symmetry comparison of all the equivalent probes. This procedure is limited by the presence of toroidal asymmetries in the measured magnetic field, due to the plasma or imposed by the surrounding structures, and when less than three probes are available, as it is impossible to distinguish the culprit probe. Accepting these limitations, this method can be expressed by the following equation:

$$\forall j, k \in O_i \colon j \neq k \wedge \|P_{i,j} - P_{i,k}\| < \varepsilon_i \tag{1}$$

where i is the equivalent probe index, $O_i \subseteq \{1, \ldots, 8\}$ is the subset of JET octants where the equivalent probes are installed, P is the calibrated probe measurement and ε_i is the maximum acceptable difference between two signals. This formula can be further improved in order to provide compensation against the toroidal mode numbers $n = 1$ and $n = 2$, by constraining O_i to the subset where the chosen octants are immune to the given mode. Moreover, a way of detecting the toroidal modes must also be available.

In the current shape controller architecture the presence of large toroidal modes has severe implications in the plasma boundary control. An example is shown in Fig. 3, where the error field correction coils (EFCC) controller [11] drives an $n = 2$ mode for a bounded period of time. In octants 3 and 7 the shape is as expected but in the octants located at $\pm 90°$ with respect to these, the plasma touches the outer wall. The problem is that the shape controller assumes a perfect axisymmetry of the plasma, with the consequence that a reliable boundary control can only be assumed in the octant selected as input to the feedback system.

As it was already introduced, the XLOC algorithm provides a valid flux map of the vacuum region. Using this information, it is possible to infer the expected value of the measured field at the location of a probe, so that a validation formula can be expressed as:

$$\forall j \in X \colon \|\psi_{m_i} - \psi_{xloc_{i,j}}\| < \varepsilon_i \tag{2}$$
$$\forall j \in X \colon \|\frac{\psi_{m_i} - \psi_{xloc_{i,j}}}{\psi_{xloc_{i,j}}}\| < \xi_i$$

where i is the index of the probe to be tested (among all the JET probes), $X \subseteq \{1, \ldots, 8\}$ is the subset of XLOC instances running in parallel, ψ_{m_i} is the measured flux for probe i, $\psi_{xloc_{i,j}}$ is the expected flux as returned by the XLOC instance j and ε_i and ξ_i are the maximum absolute and relative error thresholds. In order to be robust against the presence of toroidal modes, this method assumes that each XLOC instance maximises the number of probes from a single octant, so that j can be defined as the octant number of the majority of the probes used as an input to the XLOC algorithm. Although this can be made true for almost all the probes, there are some exception where probes from contiguous octants have to be used due to the unavailability of probes in a given region of an octant. The most common limitations are the probes installed in the poloidal limiters and in the divertor region. The presence of toroidal modes must be accepted as a limitation of the method and taken into account in the definition of the absolute and relative thresholds.

It should also be noticed that since some of the probes that are being validated are also inputs to the XLOC algorithm, as soon as a probe is declared as invalid, by a valid instance of XLOC, all the algorithm instances where the probe was being used as input can no longer be exploited until the end of the experiment. One way of overcoming this problem is to replace the faulty instance in the faulty XLOC by a synthetic probe, generated by a different XLOC, or to interpolate its value based on the values provided by neighbouring probes [12].

A final validation method can be developed by assuming that a faulty coil used as an input to an XLOC model will generate an abnormal shape. Comparing the reconstructed shape, defined as a collection of gaps, in several octants enables to assert the validity of a given XLOC reconstruction and can be expressed as:

$$\forall j, k \in O_i \colon j \neq k \wedge \|\delta_{i,j} - \delta_{i,k}\| < \varepsilon_i \tag{3}$$

where i is the gap index, $O_i \subseteq \{1, \ldots, 8\}$ is the subset of octants where the Felix-XLOC is running, δ_i is the gap value measured in meters and ε_i is the maximum allowable gap error, also expressed in meters. As before, the number of octants in the subset will be further constrained by the presence of toroidal modes. It should be noticed that this method does not individuate the culprit sensor which must be inferred by another method or by an offline evaluation.

The symmetric, XLOC and shape error methods can be applied in a real-time system in order to validate all the JET probes so that in case an important measurement is lost, action can be taken by the feedback systems to safely terminate the plasma pulse.

4. MAGNETICS VALIDATION DESIGN

4.1. RTDN

The less intrusive way of introducing a new system is by adding an external data consumer to the real-time network. As depicted in Fig. 4 the validation system would receive the magnetics data from the KC1D and KC1E systems and propagate a set of validation signals to RTPS.

Moreover the system would also publish in the RTDN the XLOC coefficients for 2 different octants and the value of the standard JET gaps in the same octants, so that a more centralised instance of the algorithm can exist. Associated with each XLOC reconstruction a single bit validation flag allows the protection system to can take action when an invalid model is being used by a critical feedback system. For each probe the validation parameters will have to be individually calculated and set.

Using valid XLOC data slave systems can calculate geometrical parameters using valid and consistent flux data. The major exception is the shape controller system, as adding an extra hop due to having XLOC running in a separator system would introduce an unacceptable delay ($> 2ms$) in the control system. Nevertheless, after receiving a request for a blind stop from RTPS due to an essential probe being faulty in one of the feedback octants, the shape controller is already capable of using a very limited set of hardwired magnetic signals to try to terminate the plasma. The magnetics validation system should also send a validation table with all the probe status so that the vertical stabilisation system can remove any faulty probe from the plasma velocity estimation input and try to guarantee the plasma vertical stability until the end of the experiment.

A further limitation of this solution is that since, for a given probe, KC1D and KC1E only send an octant at a time, the compensation for $n = 2$ modes is not available. This impacts both the confidence in the validation schemes and the ability to provide XLOC coefficients from more than two octants.

4.2. NEW SYSTEM

An alternative to overcome the limitations of having limited access to the number of toroidal measurements is shown in Fig. 5 and requires the development of a new magnetics data acquisition system. The new system would use its own data acquisition to acquire all the JET magnetic data used for feedback and to propagate and validate data immune to the $n = 2$ modes. Moreover, this scheme also allows to directly send the XLOC coefficients to the shape controller system.

Having four different and independent sources of the plasma shape allows the development of new control schemes where the XLOC input source can vary over time or be selected against external events. As an example, the shape controller could be configured to select the XLOC source which provides the smallest gaps, in given locations, for a bounded duration of time. This would guarantee that shapes driven by modes generated by the EFCC (see Fig. 3) would always be limited by the safest control input assumption. It also allows to safely switch into an alternative

XLOC source if a fault develops in one of the essential sensors without recurring immediately to the more draconian blind stop.

4.3. HYBRID SYSTEM

An hybrid alternative would consist in having a new data acquisition system writing to the real-time network the values from four different octants and using an independent validation system (as in the RTDN based design). Although this would allow to reject $n = 2$ modes, it has the major limitation of not allowing its outputs to be directly used by the feedback systems, as it adds an extra latency hop to the control loops, critical in particular to the plasma position and shape control.

5. PROTOTYPE

A real-time prototype was developed in order to assess the expected performance of a magnetics validation system. The prototype was developed using the MARTe [13] framework with the following main modules:

- input data source feeding the real-time chain with JET experimental data from old pulses;
- compensation of all the magnetic signals against toroidal field pickup;
- four Felix-XLOC instances, each with input probes mainly from octants 1, 3, 5 and 7.

For each real-time cycle, each Felix-XLOC computes the expected flux at the poloidal location of more than 100 probes and calculates approximately 40 gaps. This information is stored and retrieved at the end of the simulated experiment, in order to be fed into a series of scripts implementing equations 1, 2 and 3.

The script starts by detecting the presence of an $n = 1$ or $n = 2$ mode by comparing the measured value of four saddle coils, located in the same poloidal location but in different octants, so that an $n = 1$ exists if:

$$S101(k) + S701(k) - S301(k) - S501(k) > T(n = 1) \tag{4}$$

and equivalently for an $n = 2$:

$$S101(k) + S501(k) - S301(k) - S701(k) > T(n = 2) \tag{5}$$

where S101, S301, S501 and S701 are the measured value of the saddle coils located in the poloidal position 1, in the octants 1, 3, 5 and 7, respectively, at the instant k, and $T(n = 1)$ and $T(n = 2)$ are two threshold values set to 0.1.

The subset of octants O_i and X used in equations 1, 2 and 3 is updated accordingly to the detection of a mode. This means that while a mode is present if there are not enough toroidally distributed measurements to validate the probe, it is assumed that the probe is working during this period of time. Clearly the major limitation of this method is when an healthy probe develops a fault while a mode is present.

A probe is considered to be faulty if the relations in equations 1 and 2 hold simultaneously for the relative and absolute errors cases. Furthermore, this inequality must be asserted during a consecutive period of time, set to four samples. The error threshold settings vary with the class of probes used, as too restrictive values generate a large amount of false positives. The selected absolute values varied between 10% and 30% of the maximum sensor value and the relative value between 20% and 30%. An XLOC reconstruction is deemed to be invalid when either a faulty sensor is used as an input to the model or when equation 3 does not hold.

5.1. RESULTS

The simulations were performed on a 6 core AMD PhenomTM II X6 1090T 3.2 GHz processor, running Linux with isolated cores. This technique disallows the Linux scheduler from executing standard tasks in the isolated cores, guaranteeing that fully dedicated processing power is allocated to the real-time tasks. As shown in Fig. 6 the execution time of all the four XLOC instances is bounded to 800 μs, asserting the real-time capability of the system.

The validation algorithms were checked against different experiments, in order to understand the number of false positives and missed detections. Some JET sensors are known not to work but these are obviously not used as input to the reconstruction algorithms. The time it takes the validation algorithms to detect the sensor fault is also a very important measurement, in particular when these are used in a closed feedback control scheme.

The algorithms were tested in high plasma current experiments (e.g. #79698), in pulses with large vertical displacements triggered by plasma disturbances and kicks [14] (e.g. #78442) and in the JET pulses #77335 and #82467 where the EFCCs were used to produce an $n = 1$ mode and $n = 2$ mode, respectively. The validation algorithms did not trigger any false positives and successfully detected all the existent faulty sensors before the start of the plasma.

When tested in a pulse where a faulty probe was used by one of the XLOC models, as depicted in Fig. 7, the algorithms did fail to identify the culprit sensor, but triggered a false positive in a different sensor due to an erroneous prediction of the model where the probe was being used as input. Moreover, the generated plasma shape had a strong asymmetry, with respect to shape predicted by the other models, in some of the gaps. If the detection mechanism was available in this experiment, the model would have been correctly invalidated and protection action triggered.

In order to study the open-loop reaction of the system due to a fault in one of the sensors used by the models in a high current plasma pulse (#79698), as shown in Fig. 8, three types of likely problems were simulated in a crucial probe (IDC 1 of octant 3). The first fault consists of a sudden short circuit, the second of an erroneous compensation factor, adding a constant bias, and the third of a variable compensation factor. All the faults were triggered at $t = 10\ s$ when the plasma current was near its maximum value.

The simulations were run using two XLOC models, corresponding to the RTDN only design, and using four XLOC models, taking also advantage of the availability of up to four equivalent values for some of the probes. As illustrated in Fig. 9 it is clear that although all the faults are successfully detected in both cases, the latter allows for a much more expedite detection. One reason is that with only two octants available the output of equation 1 cannot be used, since it is impossible to distinguish the culprit of a possible imbalance. Moreover, having four reconstructed values greatly increases the likelihood of detecting the fault. The four XLOC version detected all the simulated faults within 28 samples (with 4 assertion samples), equivalent to 56 ms. Nevertheless, when compared to the only real situation, i.e. pulse #80912, both systems required 93 samples (186 ms) to trigger the fault.

In order to assess the possibility of using a difference in the plasma shape, defined as the error between the value of key gaps produced by all the different models, the algorithm was tested against the same real and simulated pulses discussed above. As depicted in Fig. 10, a noticeable gap error is developed when a faulty probe is used by a model.

6. CONCLUSIONS

This work discusses three alternative designs for the detection of faulty probes in the JET tokamak. Having such a system increases the overall safety of the device and guarantees that validated data is always used by the plasma control systems that rely in the magnetics diagnostic data.

The validation schemes take advantage of the toroidal symmetry of some probes and on the reconstructed probe and shape values as computed by XLOC models. These algorithms were asserted against a large variety of real and simulated scenarios always enabling the detection of the faulty probes. In order to be able to reject toroidal non-axisymmetric modes the system requires the execution of distributed XLOC models which maximise the number of probes from a given toroidal angle. It was shown that the greater the number of models available, the faster the detection.

All the three proposed designs are based on JET standard components: RTDN real-time network, multi-core computers with isolated cores and the MARTe real-time framework. It was also assumed that as soon as a fault is detected, the respective model can be invalidated and that a protective and conservative reaction can be triggered in order to try to safely land the plasma. In future fusion devices, where the plasma power and duration is expected to be significantly higher, new mechanisms which enable the live replacement of the faulty probes will have to be assessed. Moreover, the status of the magnetic boundary reconstruction can also be used to trigger other shape controlling strategies such as the position reflectometer presented in [15].

ACKNOWLEDGMENT

This work was supported by the European Communities under the contract of Association between EURATOM/IST and was carried out within the framework of the European Fusion Development Agreement. The views and opinions expressed herein do not necessarily reflect those of the European Commission.

REFERENCES

[1] F. Sartori, A. Cenedese, and F. Milani, “JET real-time object-oriented code for plasma boundary reconstruction,” *Fusion Engineering and Design*, vol. 66-68, pp. 735 – 739, 2003, 22nd Symposium on Fusion Technology.

[2] V. D. Shafranov, “Equilibrium of a toroidal plasma in a magnetic field,” *Journal of Nuclear Energy. Part C, Plasma Physics, Accelerators, Thermonuclear Research*, vol. 5, no. 4, p. 251, 1963.

[3] L. Zabeo, G. Artaserse, A. Cenedese *et al.*, “A new approach to the solution of the vacuum magnetic problem in fusion machines,” *Fusion Engineering and Design*, vol. 82, pp. 1081–1088, 2007.

[4] A. Stephen, G. Arnoux, T. Budd, P. Card, R. Felton, A. Goodyear, J. Harling, D. Kinna, P. Lomas, P. McCullen, P. Thomas, I. Young, K.-D. Zastrow, D. Alves, A. Neto, S. Devaux, and S. Jachmich, “Centralised coordinated control to protect the JET ITER-like wall,” in *13th International Conference on Accelerator and Large Experimental Physics Control Systems (ICALEPCS’11)*, 2011.

[5] R. Felton, K. Blackler, S. Dorling *et al.*, “Real-time plasma control at JET using an ATM network,” in *Proceedings of the 11th IEEE NPSS Real Time Conference*, 1999, pp. 175 –181.

[6] A. Pironti and M. Walker, “Fusion, tokamaks, and plasma control: an introduction and tutorial,” *IEEE Control Systems Magazine*, vol. 25, no. 5, pp. 30–43, 2005.

[7] F. Sartori, G. De Tommasi, and F. Piccolo, “The joint european torus, plasma position and shape control in the world’s largest tokamak,” *IEEE Control Systems Magazine*, vol. 26, no. 2, pp. 64–78, 2006.

[8] A. Cenedese, F. Sartori, V. Riccardo, and P. Lomas, “JET first wall and divertor protection system,” *Fusion Engineering and Design*, vol. 66–68, no. 0, pp. 785 – 790, 2003.

[9] D. Mazon, J. Blum *et al.*, “Real-time identification of the current density profile in the JET tokamak: method and validation,” in *Decision and Control, 2009 held jointly with the 2009 28th Chinese Control Conference. CDC/CCC 2009. Proceedings of the 48th IEEE Conference on*, dec. 2009, pp. 285 –290.

[10] A. Batista, A. Neto, M. Correia, A. Fernandes, B. Carvalho, J. Fortunato, J. Sousa, C. Varandas, F. Sartori, and M. Jennison, “ATCA control system hardware for the plasma vertical stabilization in the JET tokamak,” *Nuclear Science, IEEE Transactions on*, vol. 57, no. 2, pp. 583 –588, april 2010.

[11] D. Alves, R. Vitelli, L. Zaccarian, L. Zabeo, A. Neto, F. Sartori, P. McCullen, and P. Card, “The new error field correction coil controller system in the joint european torus tokamak,” Fusion Engineering and Design, vol. 86, no. 6–8, pp. 1034 – 1038, 2011.

[12] R. Nouailletas, P. Moreau, and S. Bremond, “A generic method for real time detection of magnetic sensor failure on tokamaks,” Fusion Engineering and Design, vol. 87, no. 3, pp. 289 – 297, 2012.

[13] A. C. Neto, F. Sartori et al., “MARTe: A multiplatform real-time framework,” Nuclear Science, IEEE Transactions on, vol. 57, no. 2, pp. 479 –486, april 2010.

[14] E. de la Luna et al., “Magnetic ELM triggering using the vertical stabilization controller in JET,” in Proc. 36th EPS Conf. on Plasma Phys., Sofia, Bulgaria, Jun. 2009.

[15] J. Santos, L. Guimarãis,M. Zilker,W. Treutterer,M.Manso, and the ASDEX Upgrade Team, “Reflectometry-based plasma position feedback control demonstration at ASDEX Upgrade,” Nuclear Fusion, vol. 52, no. 3, p. 032003, 2012.

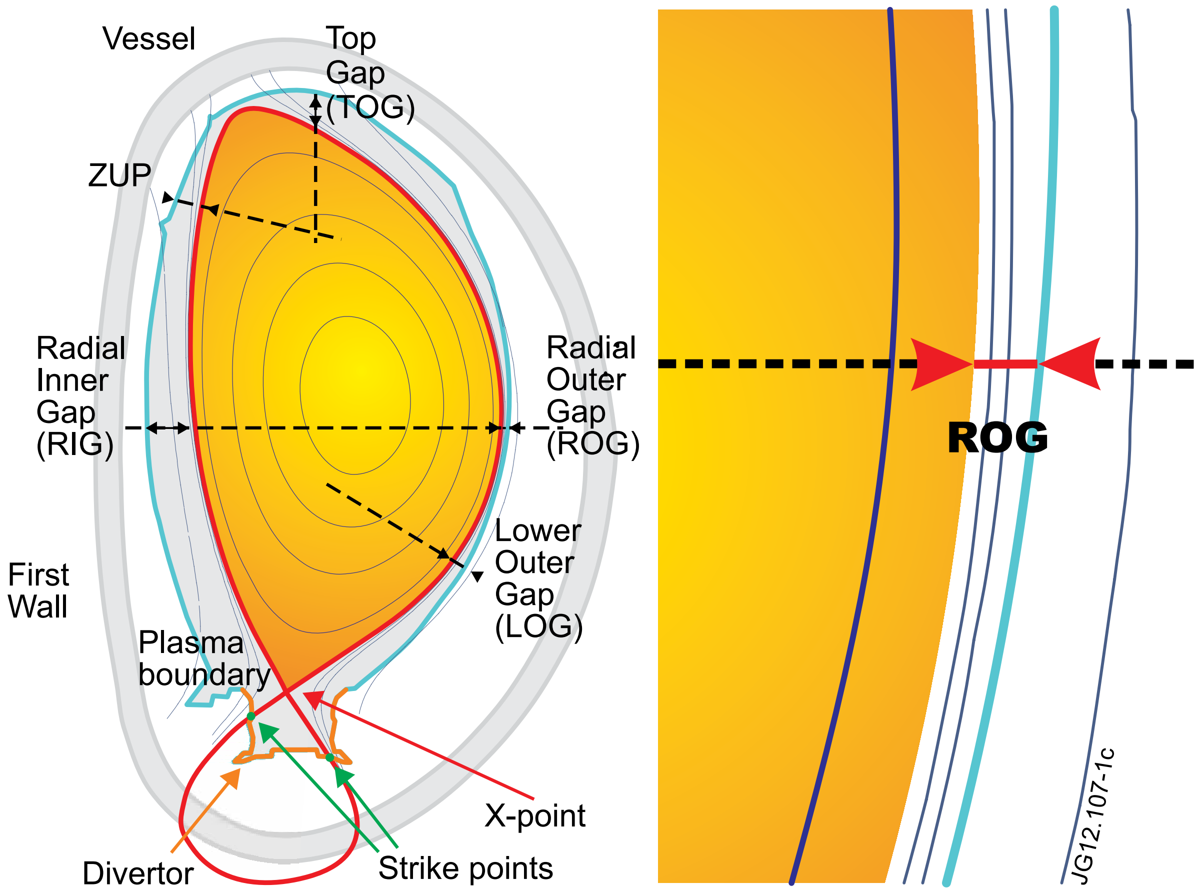

Figure 1: The plasma last closed flux surface can be defined by physical limiter in the first wall of the machine or by a magnetic configuration with an X-point ($B_r = B_z = 0$). Having a flux map it is possible to define a plasma shape as the distance to a given reference along predefined paths, also known as gaps.

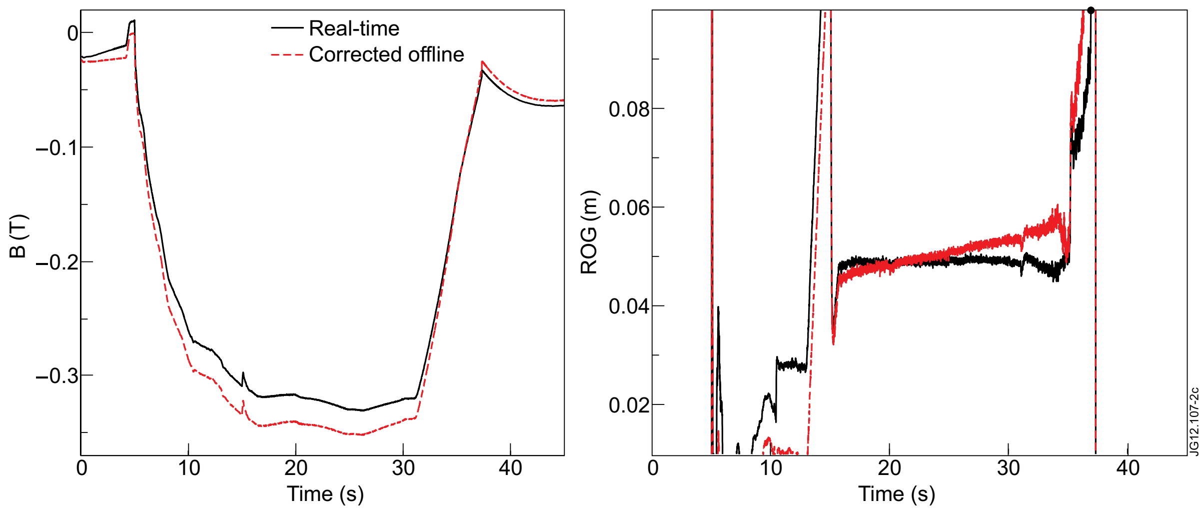

Figure 2: Data from JET Pulse No: 80912, where a software fault in the magnetics diagnostic generated a wrong compensation in the P804A coil value sent in real-time (left figure). This translated into an erroneous control of the horizontal distance to the first wall (right figure) in the order of 1cm.

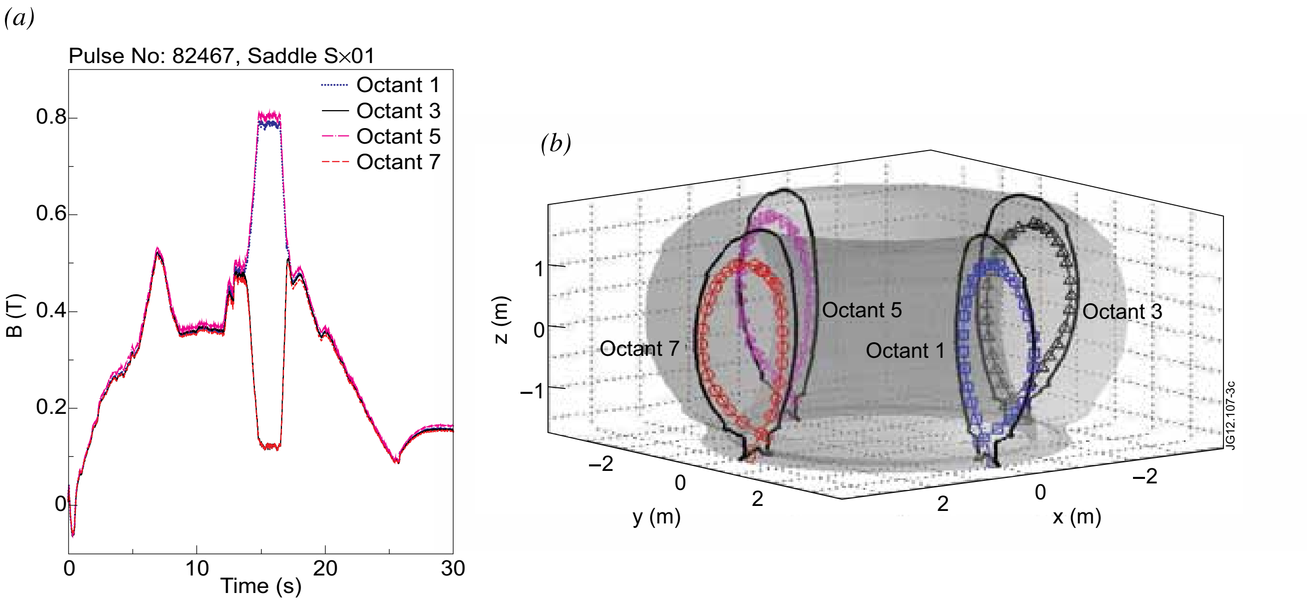

Figure 3: In the JET Pulse No: 82467 at 2 15 s the EFCC controller is enabled and generates an n = 2 toroidal mode. As a consequence the axisymmetric assumption for plasma shape control is no longer valid and drives the plasma to touch the outer wall in octants 1 and 5.

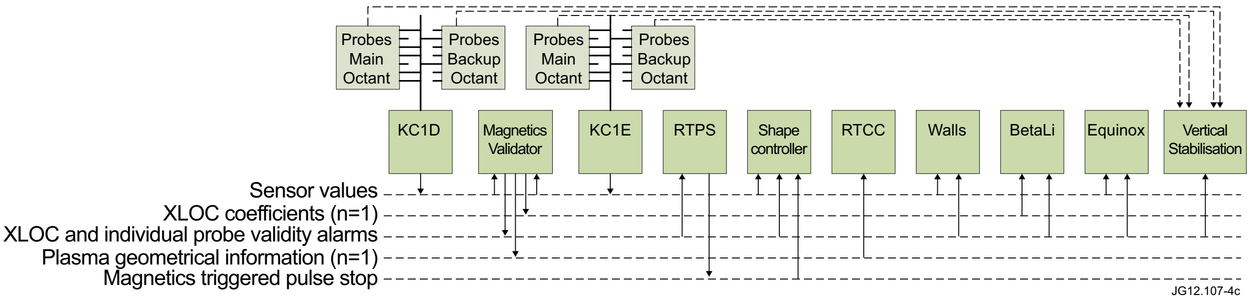

Figure 4: Validation architecture with minimum impact in the current infrastructure. The magnetics validator receives the magnetic data from the KC1D and KC1E existing systems and generates two flux maps with the associated validation information. Based on the validation flags of each XLOC reconstruction the RTPS system is capable of issuing an early termination of the experiment.

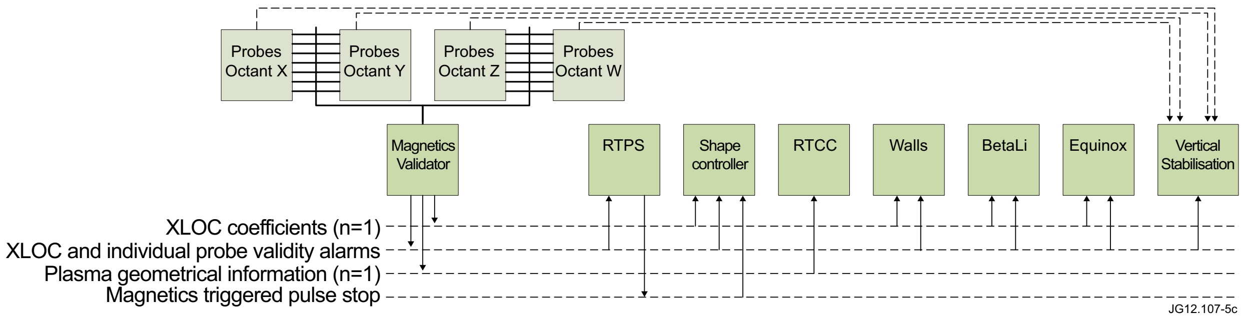

Figure 5: This architecture requires the development of a new data acquisition system, but enables full access to all the relevant JET magnetic sensors. Using this information n = 2 validated data would be available and could be directly used by the shape controller system.

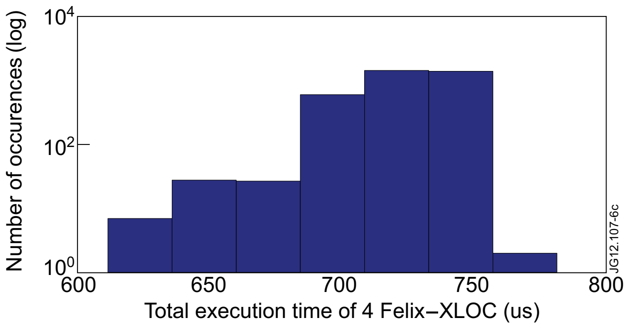

Figure 6: All the four XLOC instances execute within 800μs. Each computes more than 100 field measurements at the probe locations and outputs the plasma shape with a resolution of 40 gaps.

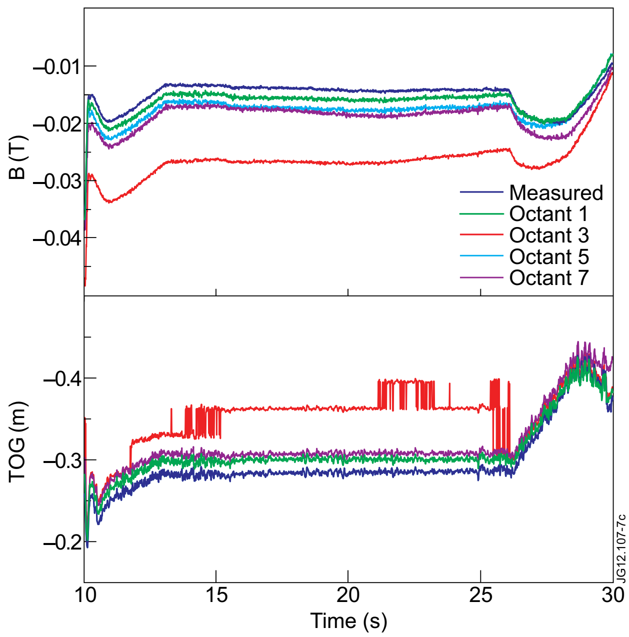

Figure 7: In JET Pulse No: 80912 a faulty probe was used by the XLOC model (Octant 3) which generates the boundary shape for control. If the algorithms were available at the time a fault would have been triggered by an asymmetry in the shape (bottom) and a false positive in a working sensor (top).

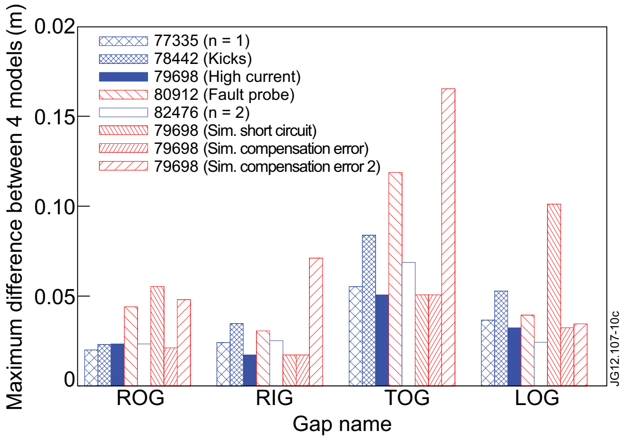

Figure 8: Three types of faults were simulated by changing the value of an XLOC probe from t = 10s. The compensation error are equivalent to adding a constant and a variable bias.

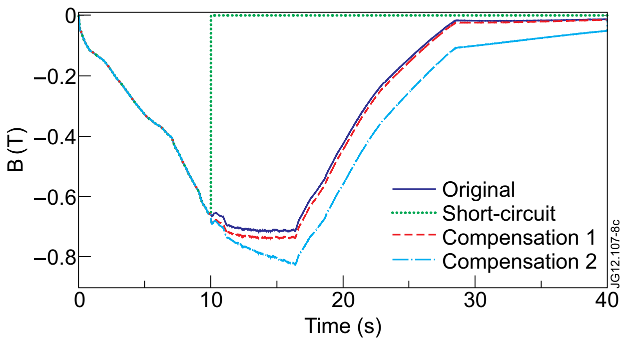

Figure 9: Using four XLOC models greatly increases the likelihood of detecting the fault. The four XLOC version detected all the simulated faults within 28 samples, equivalent to 56ms.

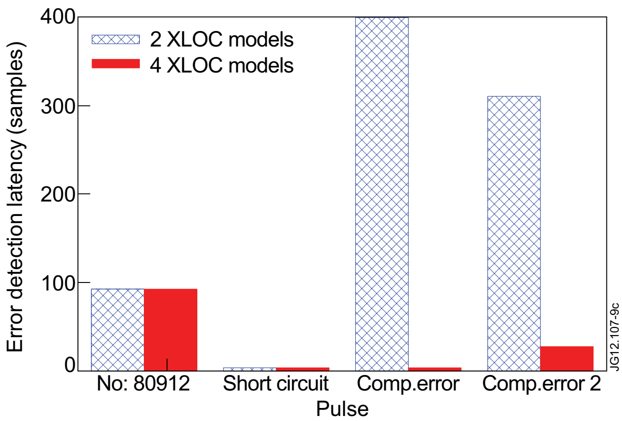

Figure 10: Maximum difference between the gaps produced by each model. When a faulty probe is used by one of the models at least one noticeable gap error difference is developed and can be used to trigger a fault.